Preparation and Characterization of Ultraviolet-Curable Nanocomposite Coatings Initiated by Benzophenone/*n*-Methyl Diethanolamine

Fusheng Li,[1] Shuxue Zhou,[1] Guangxin Gu,[1] Bo You,[1] Limin Wu[1,2]

[1]*Department of Materials Science, Advanced Coatings Research Center of Chinese Educational Ministry, Fudan University, Shanghai 200433, People's Republic of China*
[2]*College of Chemistry and Materials Science, Hubei University, Wuhan 430062, People's Republic of China*

Received 7 June 2004; accepted 2 September 2004
DOI 10.1002/app.21538
Published online in Wiley InterScience (www.interscience.wiley.com).

ABSTRACT: A series of ultraviolet-curable nanocomposite coatings were prepared with condensed nanosilica particles and with benzophenone/*n*-methyl diethanolamine as the initiator. The nanosilica that incorporated into the nanocomposites did not aggregate even when the nanosilica concentration was as high as 22.5%. Adding nanosilica increased the curing speed, thermal stability, and ultraviolet shielding properties of the nanocomposites without reducing the transparency of the ultraviolet-curing coatings. © 2005 Wiley Periodicals, Inc. J Appl Polym Sci 96: 912–918, 2005

Key words: kinetics (polym.); nanocomposites; photopolymerization

INTRODUCTION

Nanocomposites, novel composite materials with a dispersed ultrafine phase (1–100 nm),[1–5] show very interesting properties that are dramatically different from those of conventional composites. As a subdivision of nanocomposites, ultraviolet (UV)-curable nanocomposites combine the advantages of the UV-curing process and nanotechnology and therefore possess some unique properties;[6–9] they are widely used in coatings, printings, inks, adhesives, and other applications.[10–12]

On the basis of the state of the added nanosilica particles, the preparation processes of UV-curable nanocomposites can be classified into two categories: nanosilica in powder[13,14] and nanosilica in sol.[15] High purity is the main advantage of nanosilica powder, but there is an upper limit, usually 3 wt %,[13] for the embedded nanosilica concentration, and most of the properties of nanocomposites cannot be improved at such a low nanosilica concentration. As for nanosilica sol, the nanosilica concentration in nanocomposites can reach 35 wt % or even higher.[14] However, nanosilica sol will unavoidably bring impurities such as water and ethanol (EtOH), which may ultimately affect the long-term properties of UV-cured materials.

Because of the drawbacks of these two methods, a new process, illustrated in Figure 1, is proposed, in which the nanosilica sol is condensed *in vacuo* before its addition so that impurities such as water and EtOH can be excluded. With our proposed method, a series of nanocomposites with different nanosilica concentrations were prepared, and their UV-curing kinetics, microstructures, and properties were investigated with Fourier transform infrared (FTIR) spectroscopy, transmission electron microscopy (TEM), and thermogravimetric analysis (TGA), respectively.

EXPERIMENTAL

Materials

Tetraethyl orthosilicate (TEOS) and 3-(trimethoxysilyl) propyl methacrylate (MPS) were both purchased from Shanghai Huarun Chemical Co. (Shanghai, China). *n*-Butyl acetate (Analytical pure-grade), absolute EtOH, and an ammonia solution (25–28% ammonia) were purchased from Shanghai Chemistry Reagent Co., Ltd. (Shanghai, China). *n*-Methyl diethanolamine (MDEA) and benzophenone (BP) were provided by Changzhou Wujin Chemical Factory

Correspondence to: L. Wu (lxw@fudan.ac.cn).
Contract grant sponsor: National 863 Foundation.
Contract grant sponsor: Shanghai Special Nano Foundation.
Contract grant sponsor: Doctoral Foundation of University.
Contract grant sponsor: Trans-Century Outstanding Talented Person Foundation of the Chinese Educational Ministry.
Contract grant sponsor: Key Project of the Chinese Educational Ministry.

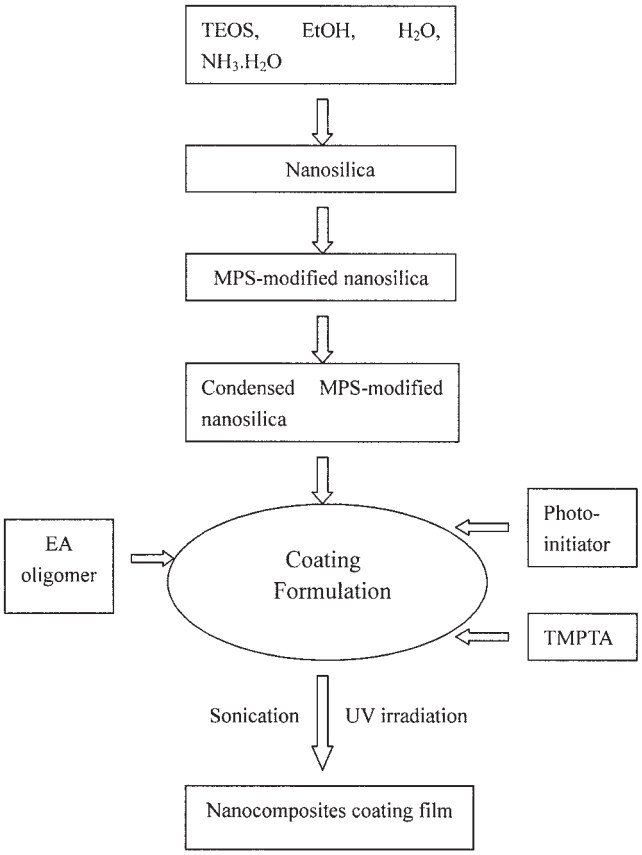

Figure 1 Schematic diagram of the process for preparing the nanocomposites.

(Changzhou, China). Trimethylolpropane triacrylate (TMPTA) and epoxy acrylate (EA; oligomers; weight-average molecular weight = 1000) were products of Sanmu Corp. (Yixing, China). All these materials were used without further purification.

Preparation and modification of the colloidal silica microspheres

Colloidal silica microspheres with an average size of 40 nm were prepared according to ref. 13. The EtOH/NH_3/H_2O/TEOS molar ratio was 9:0.2:2.5:1. In brief, TEOS and partial absolute alcohol were first charged into a three-necked, round-bottom flask, and then the residual absolute alcohol, deionized water, and ammonia were added via dropping within 0.5 h; the mixture reacted for 24 h with stirring. Then, MPS was added in a 3:14 (w/w) MPS/TEOS ratio, and the reaction continued for another 6 h. The resultant nanosilica sol was condensed *in vacuo* at 50°C to remove all the water and EtOH. Finally, a liquid mixture of MPS-modified nanosilica particles and residual MPS was obtained for further use.

Preparation of the EA/SiO_2 nanocomposites

The condensed nanosilica was added to TMPTA, and the mixture was treated with ultrasonication for 30 min and added to the EA oligomeric resin. This mixture was ultrasonicated for another 30 min, and this was followed by the addition of BP and MDEA. The formulations are summarized in Table I. The nanocomposite coatings were prepared by the casting of the aforementioned solution onto glass substrates and were cured with the UV irradiation of a mercury lamp (1 kW and maximal irradiation at a wavelength of 365 nm) at various conveyer speeds in air.

Characterization of the nanosilica particles and nanocomposites

FTIR

The IR spectra of the samples before and after UV curing were scanned with a Magna IR 550 spectrometer (Nicolet Instruments, Madison, WI). In the UV curing kinetics study, a sandwich-like NaCl plate was used for the FTIR scanning to minimize the influence of oxygen in the atmosphere because oxygen could easily influence the curing process investigated with FTIR. The nanosilica powder used for the FTIR characterization was the product centrifuged from the MPS-modified nanosilica sol.

TEM

TEM micrographs were taken with an H-600 apparatus (Hitachi Corp., Tokyo, Japan). The samples were prepared with an ultramicrotome at room temperature, which produced sections nearly 100 nm thick. No further staining was used to improve the contrast. The image analyses were performed with Photoshop 7.0 software installed on a personal computer.

TGA

The TGA curves were obtained with a thermogravimetric apparatus (SDT 2960, TA Instruments, New Castle, DE). The temperature ranged from room tem-

TABLE I
Formulations for the Preparation of the EA/SiO_2 Nanocomposite Coatings

Sample code	Formulation (g)					SiO_2 (%)[a]
	EA	TMPTA	Condensed SiO_2 Sol	BP	MDEA	
A	40	55	0	3.2	2.2	0
B	40	50	5	3.2	2.2	2.5
C	40	45	10	3.2	2.2	5
D	40	40	15	3.2	2.2	7.5
E	40	25	30	3.2	2.2	15
F	40	10	45	3.2	2.2	22.5

[a] Based on the total solid mass content.

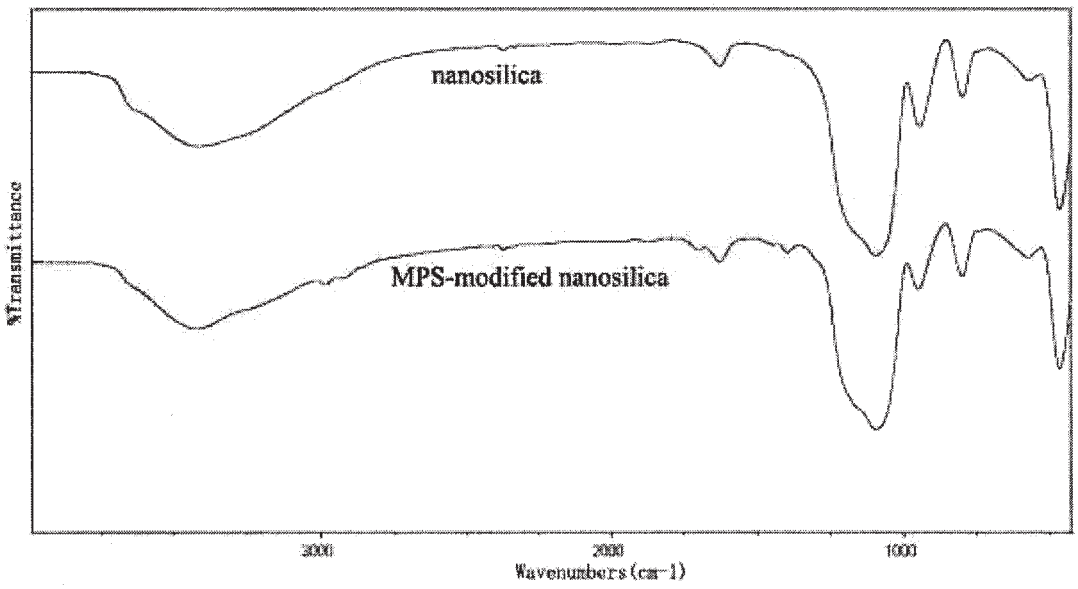

Figure 2 FTIR spectra of unmodified nanosilica and MPS-modified nanosilica particles.

perature to 900°C at a heating rate of 10°C/min in the air flow.

Ultraviolet–visible (UV–vis) spectroscopy

The absorbance and transmittance spectra of the nanocomposite films at light wavelengths of 190–700 nm were recorded with a UV–vis spectrophotometer (UV-3000, Hitachi).

RESULTS AND DISCUSSION

Preparation of the MPS-modified nanosilica particles by the sol–gel method

The size of the nanosilica particles prepared in our laboratory was 40 nm according to TEM observations with 9:0.2:2.5:1 (mol/mol/mol/mol) EtOH/NH_3/H_2O/TEOS.[13] Because nanosilica particles prepared by the sol–gel method are usually hydrophilic and tend to aggregate in organic dilutions or polymers, their applications to organic polymers are greatly restricted. Therefore, it is very necessary to modify colloidal silica particles with some hydrophobic compounds, such as MPS. The FTIR spectra of MPS-modified nanosilica powders and nanosilica without modification are shown in Figure 2. With respect to the spectrum of the unmodified nanosilica particles, a new absorption peak at 1730 cm^{-1}, assigned to a C═O vibration, can be observed in the spectrum of the MPS-modified nanosilica particles, and it indicates that MPS was successfully attached to the surface of the nanosilica particles. The resultant MPS-modified nanosilica sol was then condensed *in vacuo* at 50°C to remove almost all water and EtOH because water and EtOH molecules are usually very detrimental to both the UV-curing process and final coating properties.[16]

Photopolymerization kinetics of the nanocomposites

Typical FTIR spectra of UV-curable nanocomposite coatings with different irradiation times are illustrated in Figure 3. The intensity of the peak at 1635 cm^{-1} for the C═C stretching absorbance decreased with increasing exposure time under UV irradiation. Because the peak at 1635 cm^{-1} is well separated from other peaks, it is usually used to quantify the conversion of C═C bonds in UV-curable coatings, and another peak at 1725 cm^{-1}, due to C═O stretching absorbance, is designated as the reference peak for its invariability[17] during UV curing. Thus, the conversion of C═C bonds (C) can be calculated as follows:

$$C(\%) = 100 \times (1 - A_t S_0 / A_0 S_t) \quad (1)$$

where A_t and A_0 are the areas of the 1635-cm^{-1} peak and S_t and S_0 are the areas of the 1725-cm^{-1} peak at time t and time $t = 0$, respectively.

On the basis of the data calculated with eq. (1), conversion curves for the UV-curable nanocomposite coatings were obtained. Figure 4 demonstrates typical conversion curves for the nanocomposite coatings with 5.0 or 7.5% nanosilica and the pure polymer for comparison. The photopolymerization kinetics of the nanocomposite coatings were generally similar to those of the UV-curable coating without the nanosilica. The conversion of double bonds increased quickly at the beginning of UV curing because of the

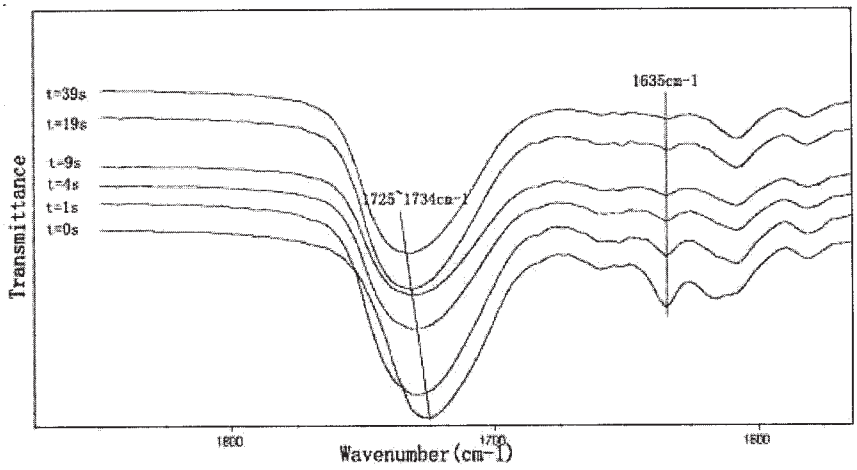

Figure 3 FTIR spectra of UV-curable coatings after different irradiation times.

high reactivity of TMPTA, and then the polymerization rate slowed down because of the vitrification of the resin. This was a typical kinetic curve for UV-curable coatings with three functional reactive dilutions.[6] Adding nanoparticles increased both the photopolymerization rate and the final conversion in comparison with those of the coating without nanosilica, and this was very surprising to us. According to our preliminary idea, because nanosilica particles can absorb UV rays,[13,18,19] they are supposed to reduce the curing rate and conversion when they are embedded in UV-curable resins. The obtained opposite results can possibly be explained as follows.

The UV-curing polymerization of multifunctional monomers is generally divided into three stages with respect to the reaction kinetics. In the first stage, the conversion quickly reaches 50% or higher within the first several seconds, the formed polymer network restricts the mobility of the radical species, the termination step becomes diffusion-controlled, and this results in an increase in the free-radical concentration and hence in the polymerization rate.[20] In comparison with the pristine polymer, the existence of an inorganic nanosilica network will accelerate this process and make this acceleration process more obvious. In other words, this process will occur at an earlier time because an inorganic network has an effect similar to that of a crosslinked organic network on the curing process.

As the reaction continues, the decreased mobility of the propagating radicals and the reduction of the number of functional groups slow down the polymerization reaction, some unreacted monomers and radicals are trapped in the UV-cured organic matrix, and so the propagation reaction becomes diffusion-controlled. In this stage, the existence of an inorganic nanosilica network in the organic matrix facilitates the diffusion of the unreacted monomers and free radicals

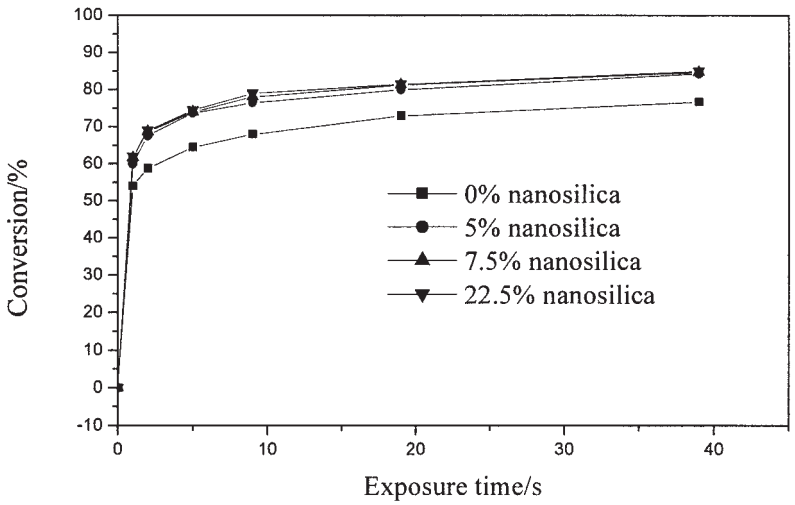

Figure 4 Conversion of UV-curable coatings versus the exposure time.

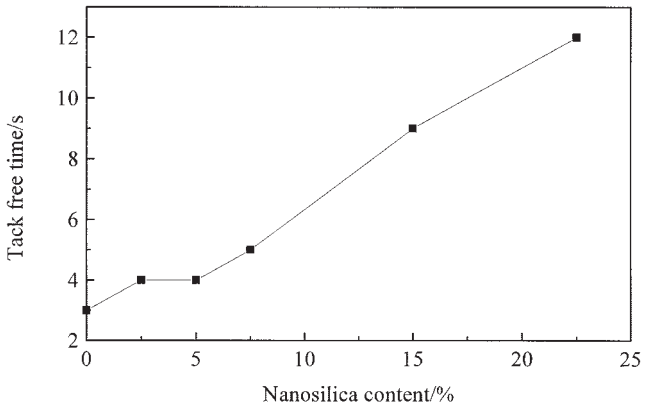

Figure 5 Tack-free time versus the nanosilica concentration for the nanocomposites.

because of the nanoscale separation of the organic phase and inorganic phase, and this alleviates the vitrification effect of the nanocomposites.[21] As a result, a higher conversion is obtained.

During the last reaction stage, most polymeric radicals are bound to the three-dimensional network and have limited mobility; therefore, the radical site will move mainly by reaction with neighboring functional groups until it combines with another radical.[20] The existence of an inorganic nanosilica network will somewhat inhibit the mobility of polymeric radicals and reduce the bimolecular termination reaction, thus prolonging the lifespan of the polymeric radicals and finally leading to a higher final conversion.

On the basis of this proposed mechanism, a higher UV-curing speed in the nanocomposites was observed in this experiment, and this was also observed by Soppera and Barghorn.[22]

Tack-free time

The tack-free time, a parameter used to characterize the curing level on the surface of a film, is usually used to evaluate the influence of nanosilica on the surface curing speed of a coating system in the presence of oxygen.[23,24] The tack-free time increased with an increasing nanosilica concentration in the nanocomposite polymers, as indicated in Figure 5; this was far beyond our expectations. Because incorporating the nanosilica particles enhanced the photopolymerization rate and the rate increased with an increasing nanosilica concentration, as indicated in Figure 4, the tack-free time was supposed to shorten. The reason that the tack-free time is extended with the addition of nanosilica may be the good permeability of oxygen in the nanosilica network due to the porous structure.[25] The higher the nanosilica content is, the more obvious this permeability effect is, the stronger the inhibition effect of oxygen to the surface polymerization of the nanocomposite film is, and thus the longer the tack-free time is.

Morphology of the nanocomposites

The transparency of the cured nanocomposite films is noteworthy. It means that no macroscopic phase separation occurred and no silica domains greater than the wavelength of visible light existed. The morphology of the nanocomposites with 2.5 and 22.5% silica concentrations, as shown in Figure 6, shows that the nanosilica particles were evenly dispersed in the polymer matrix. The diameter of the particles was very close to the particle size of the original colloidal silica (ca. 40 nm), and this implies that there was no aggregation of nanosilica particles in the preparation of the UV-curable nanocomposite coatings, even when the nanosilica concentration was 22.5%. These results contradict the conclusions reported by Zhang et al.[15] The uniform dispersion of nanosilica particles within the matrix indicates that the method of importing colloidal nanosilica particles, including MPS modification, sol condensation, and sonication, put forward in this study is feasible. After MPS modification, some C═C groups of MPS molecules attached to nanosilica particles can react with reactive dilutions or oligomers during the UV-curing process and thus further improve the compatibility of the nanosilica particles with the organic matrix.

Thermal stability of the nanocomposites

The thermogravimetric behavior of the nanocomposites with various nanosilica concentrations is shown in Figure 7. The nanocomposites containing nanosilica did not start to lose weight dramatically until 370°C, whereas for pristine EA, the decomposition onset temperature was 200°C. This indicates that the thermal stability of UV-curable coatings can be greatly improved by the addition of nanosilica particles, and this means that an inorganic nanosilica network can prevent the degradation of polymer molecules. A possible explanation is that when nanocomposites are heated, nanosilica particles immigrate to the surface of the material because of their relatively low surface potential energy.[26] The silica on the surface of the material, therefore, can serve as a heat barrier to protect the inner layer of the polymers.

Usually, the flame-retardant properties of polymeric materials can be evaluated from their char yields: high char yields imply less production of combustible compounds and low heat release.[27] The final residues of the nanocomposites were almost equal to the theoretical content of nanosilica embedded within the experimental error range, as indicated by the curves above around 550°C in Figure 7. This suggests that no flame-retardant performance for the nanocomposites could

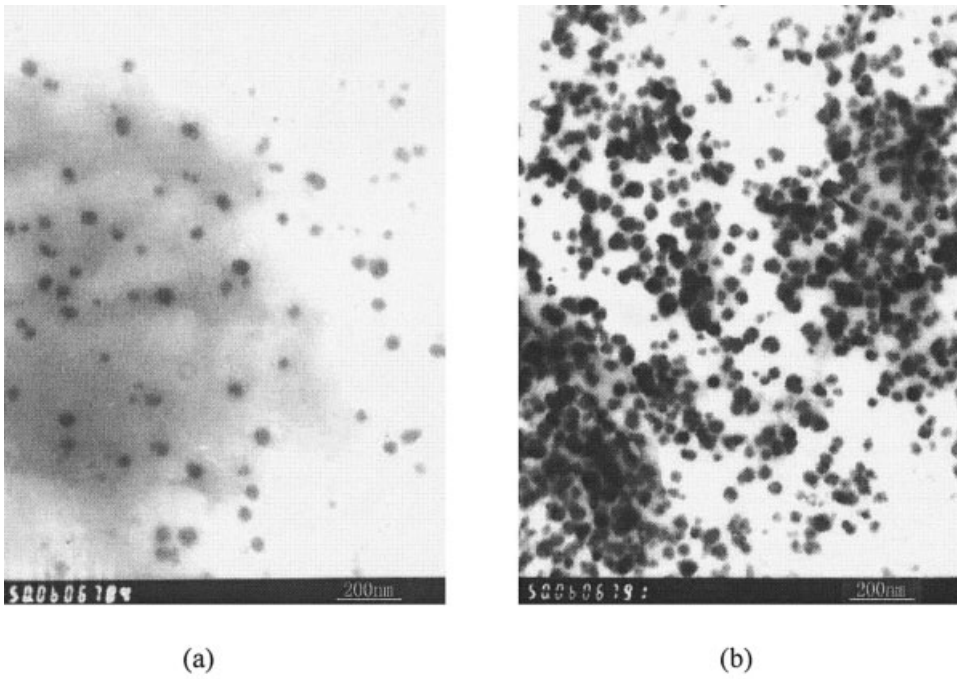

Figure 6 TEM pictures of the nanocomposites with (a) 2.5 and (b) 22.5% nanosilica.

be observed. This possibly occurred because the blending method adopted for synthesizing the nanocomposites in this study could not produce improved flame-retardant properties for nanocomposites, as proposed by Hsiue et al.[26]

Optical properties of the nanocomposites

The optical properties of nanocomposites are critical to their applications as optical fiber coatings, lens coatings, and so forth,[13] and the weather resistance of nanocomposite coatings also depends on their optical properties,[28] especially their absorbance in the UV range. Figure 8 illustrates the UV transmittance spectra of nanocomposite coatings.

At wavelengths of 400–700 nm (visible light), more than 90% of the transmittance for the pure polymer and all the nanocomposites was observed (not presented here), and this indicated that the addition of nanosilica did not reduce the transmittance of the UV-cured coatings in this wave band. However, below 400 nm, especially at 340 nm, the transmittance of the nanocomposites decreased dramatically because of the quantum size effect of the nanosilica particles. Moreover, the more nanosilica particles were embedded, the lower the transmittance was of the corresponding nanocomposites.

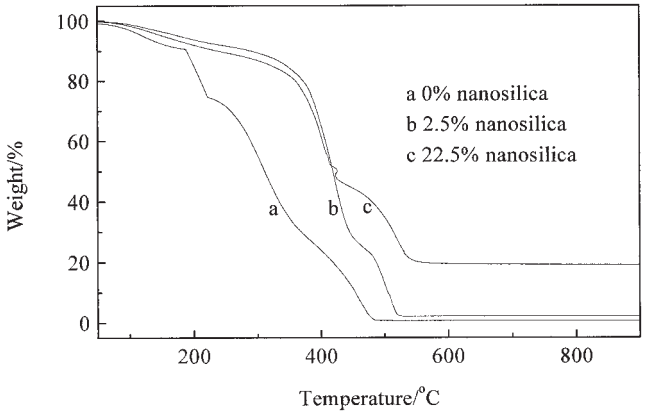

Figure 7 TGA curves of (a) the parent polymer, (b) the nanocomposites containing 2.5% nanosilica, and (c) the nanocomposites containing 22.5% nanosilica.

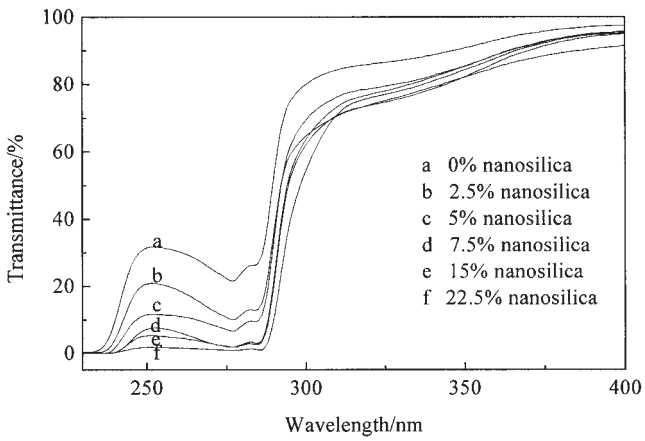

Figure 8 UV transmittance spectra of pristine EA and the nanocomposites.

To explain this phenomenon, the concept of the scattering coefficient (S) was introduced. According to the Scamatakis formula[29]

$$S = [\alpha M^3(\lambda)^{\frac{1}{2}}] / \left[\frac{\lambda^2}{2d} + n_b^2 \pi^2 M d \right] \quad (2)$$

$$M = \left(\frac{n_p}{n_b} \right)^2 - \left(\frac{n_b}{n_p} \right)^2 + 2 \quad (3)$$

where α is a constant (related to the intrinsic properties of the material); λ is the wavelength of incident light; n_p and n_b are the refractive indices of the dispersed phase and dispersed medium, respectively; and d is the particle diameter. For this system, n_p is 1.45, and n_b is 1.47. At a certain wavelength of the incident light, the maximum S value can be reached when d is $\frac{\lambda}{n_b \pi \sqrt{2M}}$. Consequently, d for the maximum scattering in the UV range of 190–400 nm is approximately 21–44 nm. Because of the small size of the nanosilica (40 nm) used in this study, the obvious reduction of the transmittance at wavelengths lower than 400 nm can be attributed to the larger S value. Therefore, the transmittance of nanocomposites in the UV range will be reduced dramatically with an increasing content of nanosilica because of its strong scattering effect. Therefore, nanocomposites reinforced with nanosilica particles can shield UV light. This outstanding transmittance and corresponding weatherability certainly bring some benefits to EA resins, especially for applications in which nanocomposites are exposed to sunlight.[28]

CONCLUSIONS

With an EA resin and TMPTA as the organic matrix, UV-curable nanocomposite coatings with different nanosilica concentrations were prepared through the addition of nanosilica in a condensed sol form. The results showed almost no aggregation of the nanosilica particles in the nanocomposites, even when the nanosilica concentration was 22.5 wt %. The curing speed of the nanocomposites was accelerated because of the existence of a nanosilica network, and the thermal stability of the nanocomposites was improved as the nanosilica concentration was increased. Meanwhile, outstanding transparency and better UV-shielding properties were obtained for the nanocomposite coatings.

References

1. Benfarhi, S.; Decker, C.; Keller, L.; Zahouily, K. Eur Polym J 2004, 40, 493.
2. Bauer, F.; Glasel, H.; Decker, U.; Ernst, H.; Freyer, A.; Hartmann, E.; Sauerland, V.; Mehnert, R. Prog Org Coat 2003, 47, 147.
3. Becker, O.; Varley, R. J.; Simon, G. P. Eur Polym J 2004, 40, 187.
4. Torre, L.; Frulloni, E.; Kenny, J. M.; Manferti, C.; Camino, G. J Appl Polym Sci 2003, 90, 2532.
5. Dong, W.; Zhu, C. Mater Lett 2000, 45, 336.
6. Bajpai, M.; Shukla, V. Pigm Resin Technol 2003, 32, 382.
7. Stowe, R. W. Met Finishing 2002, 8, 8.
8. Chao, C.; Chen, W. Chem Mater 2002, 14, 4242.
9. Mantia, F. P. L.; Verso, S. L.; Dintcheva, N. T. Macromol Mater Eng 2002, 287, 909.
10. Wenning, A. Macromol Symp 2002, 187, 597.
11. Hwang, D. K.; Moon, J. H.; Shul, Y. G.; Jung, K. T.; Kim, D. H.; Lee, D. W. J Sol-Gel Sci Technol 2003, 26, 783.
12. Oestreich, S.; Struck, D. S. Macromol Symp 2002, 187, 333.
13. Xu, G. C.; Li, A. Y.; Zhang, L. D.; Wu, G. S.; Yuan, X. Y.; Xie, T. J Appl Polym Sci 2003, 90, 837.
14. Bauer, F.; Glasel, H. J.; Hartmann, E.; Bilz, E.; Mehnert, R. Nucl Instrum Methods Phys Res Sect B 2003, 208, 267.
15. Zhang, L.; Zeng, Z. H.; Yang, J. W.; Chen, Y. L. J Appl Polym Sci 2003, 87, 1654.
16. Crivello, J. V.; Mao, Z. B. Chem Mater 1997, 9, 1562.
17. Wang, J. Z. Y.; Bogner, R. H. Int J Pharm 1995, 113, 113.
18. West, J. K.; Torre, G. L.; Hench, L. L. J Non-Cryst Solids 1996, 195, 45.
19. Zhou, S. X.; Wu, L. M.; Sun, J.; Shen, W. D. Prog Org Coat 2002, 45, 33.
20. Decker, C. Prog Polym Sci 1996, 21, 593.
21. Beiner, M.; Huth, H. Nat Mater 2003, 2, 595.
22. Soppera, O.; Barghorn, C. C. J Polym Sci Part A: Polym Chem 2003, 41, 716.
23. Bengiovanni, V. L. R.; Malucelli, G.; Priola, A.; Garavaglia, S.; Turri, A. Pigm Resin Technol 1999, 28, 212.
24. Wei, H. Y.; Lu, Y.; Shi, W. F.; Yuan, H. Y.; Chen, Y. L. J Appl Polym Sci 2001, 80, 51.
25. Rahman, M. M.; Khan, M. A.; Mustafa, A. I. J Appl Polym Sci 2002, 86, 2385.
26. Hsiue, G. H.; Liu, Y. L.; Liao, H. H. J Polym Sci Part A: Polym Chem 2001, 39, 986.
27. Liu, Y. L.; Lin, Y. L.; Chen, C. P.; Jeng, R. J. J Appl Polym Sci 2003, 90, 4047.
28. Seubert, C. M.; Nichols, M. E.; Cooper, V. A.; Gerlock, J. L. Polym Degrad Stab 2003, 81, 103.
29. Xiong, M. N.; Gu, G. X.; You, B.; Wu, L. M. J Appl Polym Sci 2003, 90, 1923.